This study considers the electromagnetic and electromechanical processes in a traction induction motor. The task addressed relates to the absence of a universal mathematical model of a high-power induction motor that accounts for magnetic circuit saturation, cross-saturation, and core losses. Such a model is required for an adequate description of transient processes under the operating conditions of marine power plants.

The essence of the results reported here is the construction of a system of equations describing the electromagnetic and electromechanical processes in a traction induction motor, taking into account magnetic circuit saturation. The proposed model includes four differential and two algebraic equations, providing complete controllability over the machine dynamics on both linear and nonlinear segments of the magnetization characteristic. By applying the dynamic inductance method, the model accounts for the interdependence between flux linkages and currents in different coordinate axes, as well as for the nonlinear variations of inductance parameters under magnetic saturation. These specific features have made it possible to accurately reproduce the real physical processes in the motor, as confirmed by bench verification based on the Caterpillar 3516 marine power plant. The results are attributed to the use of a generalized spatial model and dynamic inductances that reflect the variability of the motor's magnetic state under different load conditions.

The built model could be used in the synthesis of automatic control systems, analysis of transient processes, diagnostics of electric drives, as well as optimization of power plants. It could be practically implemented under conditions of stable thermal regime of the motor and availability of reliable experimental data for identification of saturation parameters

Keywords: induction motor, power plant, mathematical model, electromagnetic processes, dynamic inductances

UDC 621.313.33:519.87:629
DOI: 10.15587/1729-4061.2025.345066

CONSTRUCTION OF A MATHEMATICAL MODEL OF AN INDUCTION MOTOR FOR A TRANSPORT POWER PLANT INCORPORATING MAGNETIC SATURATION PROCESSES

Dmytro Kulagin
Corresponding author
Doctor of Technical Sciences, Professor
Department of Power Supply of Industrial Enterprises
Zaporizhzhia Polytechnic National University
Universytetska str., 64, Zaporizhzhia, Ukraine, 69063
E-mail: kulagindo@gmail.com

Igor Maslov
PhD, Associate Professor
Department of Marine Power Plants and Systems
Danube Institute of National University
"Odessa Maritime Academy"
Fanahoriyska str., 9, Izmail, Ukraine, 68607

Received 08.09.2025
Received in revised form 14.11.2025
Accepted 24.11.2025
Published 31.12.2025

How to Cite: *Kulagin, D., Maslov, I. (2025). Construction of a mathematical model of an induction motor for a transport power plant incorporating magnetic saturation processes. Eastern-European Journal of Enterprise Technologies, 6 (8 (138)), 24–35. https://doi.org/10.15587/1729-4061.2025.345066*

1. Introduction

Current development of world maritime transport is characterized by the transition to using electric vessel propulsion systems, in particular, electric propeller drives based on induction traction motors. This is due to the need to increase energy efficiency, reliability, and environmental friendliness of vessel operation [1, 2]. In the context of growing requirements for reducing fuel consumption, reducing harmful emissions, and ensuring stable operation of power plants, there is a need to improve models and methods for analyzing electric drives [3].

Scientific research in this area is necessary because conventional mathematical models of induction motors do not fully reflect the real electromagnetic processes occurring in the machine, in particular the effect of saturation of magnetic circuits [4, 5]. To establish optimal vessel steering modes, the navigator or the autosteering system changes operation of the power plant. This is achieved by changing the control laws of the induction motor of the propeller drive (amplitude, pulse-width control, or operation with reduced rotor flux linkage) [1, 3]. In order for the auto-steering system to be effective and economical in terms of control mode, its mathematical model must accurately reflect the physical processes in the traction power transmission. Therefore, it is extremely important to take into account the effect of saturation of the magnetic circuits of the engine since it changes its parameters under different operating modes. This will make it possible to build an accurate model that could help minimize fuel or electricity consumption. Ignoring this factor may lead to inaccuracies in the calculations of operating modes, forecasting transient processes and, as a result, to ineffective engineering solutions in the design and operation of vessel electric drives.

The practical significance of such research results relates to the possibility of constructing more accurate mathematical models that will make it possible:

– to increase the reliability of computer simulation of electric propeller drives;

– to optimize electric motor control systems taking into account nonlinear characteristics;

– to reduce energy losses and increase the equipment service life;

– to increase the reliability and safety of marine transport operation.

Therefore, it is a relevant task to carry out studies aimed at constructing a mathematical model of a vessel's propeller traction induction motor taking into account the saturation of magnetic circuits.

2. Literature review and problem statement

Current studies on magnetic saturation modeling of induction machines tend to use two main methodological groups. Paper [6] considers similar models, known as mixed current-flux or flux-linkage based models, emphasizing their advantage in the context of control problems. Work [4] reports the results of studies that use polynomial experimental dependences of inductances on fluxes or currents. These models introduce nonlinear dependence of magnetic parameters into simplified spatial models [7], thereby showing their effectiveness for basic dynamic analysis.

Another group of approaches is based on field magnetic models, in particular magnetic circuits, as described in study [5]. It is shown that such an approach gives a more physically justified description of saturation and cross-saturation since it directly takes into account the geometry of the machine, similar to work [8]. However, issues related to high computational complexity and the need for detailed geometric data regarding the machine, similar to work [9], remain unresolved. The likely reason is objective disadvantages associated with resource-intensive calculations by the finite element method (FEM), the application of which underlies study [10]. Such an approach makes the corresponding iterative research methods impractical for dynamic control problems. Additional problems arise, as shown in [11], with the need to accurately identify a large number of parameters in complex multifactor models. An option for overcoming related difficulties is to use simplified but functional methods, such as the method of statistical inductances, described in particular in [12]. In the study, nonlinear processes in the magnetizing circuit of an induction machine are taken into account through the functional dependence between the flux linkage and the magnetizing current. This significantly minimizes the computational load. A similar methodology was used in [13], in which the dependence is given in the form of a table or analytical approximation.

In [14], further improvement is proposed through the method of dynamic inductances. The authors claim that this method makes it possible to accurately take into account complex magnetic phenomena, especially under modes with large currents and a wide range of fluxes, which are characteristic of transport traction induction machines. A similar approach is used in [15]; however, despite the inclusion of saturation of the paths of leakage fluxes and mutual induction between perpendicular machine contours, it requires high accuracy in determining the functions of the dependences between these parameters of the magnetic state. In addition, in study [16], the possibility of taking into account the mutual saturation is confirmed, which increases the adequacy of the model. According to [15], the method of dynamic inductances is a convenient and effective tool for describing dynamic processes while work [17] emphasizes its advantages when it is necessary to take into account the effects of saturation.

In addition, combined models (mixed current-flux) have been devised, as shown in [18], which are widely used as a compromise between accuracy and complexity. These models, as similarly demonstrated by studies [19, 20], are applied in induction machines of relay protection drives, as well as, according to [21], for induction pump motors. However, studies [19, 20] do not take into account the entire range of magnetic processes that occur in the circuits of an induction machine, which is also characteristic of paper [21]. In addition, the considered studies [19, 20] have not been verified for high-power motors. These models have also found application in bench training drives [22], bench diagnostic models [23].

Improvement of mathematical and simulation models of induction machines taking into account saturation, as shown by study [24], led to the development of various variants of static nonlinear inductances, the evolution of which is given in work [10]. A similar approach is used in [25], but it mainly focuses on improving the accuracy of estimating torque and currents under transient regimes compared to linear models, often ignoring more subtle effects. An option to overcome this limitation could be to take into account additional nonlinearities, such as cross-saturation, similar to ref. [26]. A similar approach is used in [27], in which options are developed to take into account the effects of cross-saturation, hysteresis, and frequency-dependent losses, which are critical for powerful transport installations. However, the review in [28] shows that these complex models also have high requirements for parameter identification, making their practical application difficult.

Another direction is the application of well-known devised approaches to other motor configurations, such as polyphase machines in [29]. In [30], saturation models for six- and more-phase induction machines are described. However, as the authors of [31] note in their study of a polyphase machine, there is often a lack of validation of these methods on large-power machines, especially typical for transport power plants.

As a result of our review of current papers, it can be stated that many researchers, such as in [32], introduce saturation of the main flux. Similarly, paper [33] focuses on the same aspect. But in that work, the issue of adequate and convenient for engineering calculations consideration of cross-saturation (mutual influence of fluxes) for high-power machines remains unresolved, which is especially important for motors with uneven clearance or non-standard design. The likely reason is objective difficulties associated with the complexity of the mathematical description and the need for additional experimental parameters or a magnetic circuit for identification. In addition, a significant part of the published works, in particular [24, 27], checks the models on laboratory or medium-power induction machines. This means a potentially uncertain transferability of the results to high-power rowing traction motors. The specificity of marine traction (long-term sharply changing stochastic loads, disturbances, high inertia) are not sufficiently taken into account in the experimental verification, as noted in [34].

All this allows us to argue that it is advisable to conduct a study aimed at constructing and validating a model of a high-power induction traction machine that effectively takes into account both the saturation of the main flow and cross-saturation but, at the same time, retains minimal computational complexity for implementation in control systems under conditions typical of marine traction.

For practical applications in real-time systems, methods for fast, reliable identification of saturation parameters are needed. Many works either propose complex identification systems based on a combination of FEA and bench tests, or use approximations that degrade accuracy with temperature changes, insulation aging, or magnetic properties of steels. This is due to the limited access to a complete set of experimental data for large machines, the influence of many variables (temperature, deformations, accumulation of residual magnetization).

The combination of saturation with other nonlinear processes within the same model (hysteresis, frequency losses, gap effects) remains poorly understood. Although some studies include certain additional nonlinear effects, a systematic and effective approach to simultaneously consider saturation and other nonlinear processes in models suitable for real-time control systems with high-power motors has not yet been devised. Usually, studies make a compromise between accuracy (FEA, hysteresis models) or speed (simplified nonlinearities).

The influence of the design features of the propeller motor and the mechanical system (massive shaft, gearbox, propeller) taking into account transient disturbances of the environment and the saturation of magnetic circuits is rarely considered. This is important for an adequate description of the traction modes during maneuvers.

The reasons why these issues have remained unresolved are:

– the high cost and complexity of FEA modeling of large traction machines, the need for accurate geometric and electrical parameters of each individual engine;

– a large number of interrelated parameters (temperature, hysteresis, energy losses), which complicates experimental identification under field conditions;

– the lack of public data or bench results for large marine engines due to commercial confidentiality;

– the traditional focus of researchers on real-time control problems (where the simplest possible models are required) has led to the priority of simplified nonlinear descriptions instead of more complete physical models;

– interdisciplinary barriers: a complete description of a traction engine requires the cooperation of electromechanics, fluid dynamics engineers, and materials scientists.

Based on the identified gaps in the research into induction motors, it is possible to state a general unsolved problem as the lack of a universal, numerically efficient and verified method for constructing a spatial mathematical model of a high-power traction induction motor for a vessel propulsion system. This method should simultaneously take into account the main magnetic saturation and cross-saturation of the fluxes, hysteresis, and frequency-dependent losses, as well as variable operating conditions (temperature, load duration). It is important that it be identified and verified on marine traction machines under field/bench conditions with adequate integration into the electromechanical models of a vessel.

The specified issue corresponds to the practical goal – to build a mathematical model suitable for analyzing and designing control and diagnostic systems for propeller traction motors.

In accordance with the identified unresolved issues, the purpose of our study is to construct and verify a mathematical model of a traction induction motor in a vessel's propeller. The specified model should take into account magnetic saturation and cross-saturation, suitable for use in the study of transient regimes and in the design of control systems for vessel traction drives.

The system of research on induction machines in recent years has significantly increased the understanding of the role of magnetic saturation in the modeling of induction machines and has proposed a number of approaches for including nonlinearities in the model. However, for application to vessel traction installations, there is a set of unresolved issues. These include consideration of cross-saturation in large machines, full verification on traction motors, practical methods for identifying parameters under field conditions, as well as simultaneous consideration of hysteresis and frequency losses in models suitable for real time.

3. The aim and objectives of the study

The purpose of our study is a mathematical description of a traction induction machine taking into account the saturation of magnetic circuits, suitable for practical use in automatic control systems of vessel propulsion power plants. This will allow for a proper adequacy of the mathematical model to actual physical processes.

To achieve the goal, the following tasks were set:

– to take into account the saturation of magnetic circuits in the mathematical description of the induction motor of the vessel propulsion power plant;

– to verify the model of the induction motor for a vessel propulsion power plant taking into account the saturation of magnetic circuits.

4. The study materials and methods

The object of our study is the electromagnetic and electromechanical processes in a traction induction motor.

The scientific hypothesis assumes that the construction of a specialized mathematical model of a traction induction motor could increase the accuracy of its description. The model must take into account the saturation of the main magnetic path in a wide range of changes in the mutual induction flux of the stator and rotor. It is necessary to take into account the saturation of the scattering paths and mutual induction between perpendicular circuits at significant machine currents and the combined saturation of the working flux and scattering fluxes for key engine operating modes. This would increase the adequacy of the model to real physical processes.

As initial relations, equations and systems of equations should be taken that are the most general and suitable for studying most processes in vessel power systems. The model of a three-phase induction propeller motor is shown in Fig. 1.

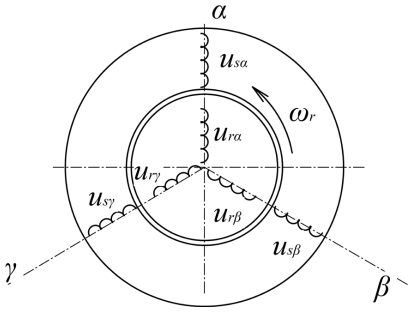

Fig. 1. Spatial model of a three-phase induction propeller motor

The statistical functional dependence between the values of flux linkage and magnetizing current is given by the following expression [4, 5]

$$\vec{\psi}_\delta = L_m\left(i_\mu\right)\vec{i}_\mu, \tag{1}$$

where $\vec{\psi}_\delta$ – generalized flux linkage vector in the air gap of an induction machine; $\vec{i}_\mu$ – generalized magnetizing current vector of an induction machine; L_μ – equivalent mutual inductance from the main magnetic field induced by the common action of the currents of all three phase stator windings of an induction machine, coupled to each phase winding of the machine, respectively.

A system of differential equations in coordinates α, β, γ, which are fixed relative to the stator [4, 5]:

$$\begin{cases} u_{s\alpha} = i_{s\alpha}\cdot r_{s\alpha} + \dfrac{d\psi_{s\alpha}}{dt}; \\ u_{s\beta} = i_{s\beta}\cdot r_{s\beta} + \dfrac{d\psi_{s\beta}}{dt}; \\ u_{s\gamma} = i_{s\gamma}\cdot r_{s\gamma} + \dfrac{d\psi_{s\gamma}}{dt}; \\ u_{r\alpha} = i_{r\alpha}\cdot r_{r\alpha} + \dfrac{d\psi_{r\alpha}}{dt} + \dfrac{\sqrt{3}\cdot\omega_r}{3}\cdot\left(\psi_{r\beta} - \psi_{r\gamma}\right); \\ u_{r\beta} = i_{r\beta}\cdot r_{r\beta} + \dfrac{d\psi_{r\beta}}{dt} + \dfrac{\sqrt{3}\cdot\omega_r}{3}\cdot\left(\psi_{r\gamma} - \psi_{r\alpha}\right); \\ u_{r\gamma} = i_{r\gamma}\cdot r_{r\gamma} + \dfrac{d\psi_{r\gamma}}{dt} + \dfrac{\sqrt{3}\cdot\omega_r}{3}\cdot\left(\psi_{r\alpha} - \psi_{r\beta}\right), \end{cases} \quad (2)$$

where $u_{s\alpha}$, $u_{s\beta}$, $u_{s\gamma}$ – projections of stator voltage vectors onto the corresponding axes α, β, γ; $u_{r\alpha}$, $u_{r\beta}$, $u_{r\gamma}$ – projections of rotor voltage vectors onto the corresponding axes α, β, γ; $i_{s\alpha}$, $i_{s\beta}$, $i_{s\gamma}$ – projections of stator current vectors onto the corresponding axes α, β, γ; $i_{r\alpha}$, $i_{r\beta}$, $i_{r\gamma}$ – projections of rotor current vectors on the corresponding axes α, β, γ; $\psi_{s\alpha}$, $\psi_{s\beta}$, $\psi_{s\gamma}$ – projections of stator flux linkage vectors onto the corresponding axes α, β, γ; $\psi_{r\alpha}$, $\psi_{r\beta}$, $\psi_{r\gamma}$ – projections of rotor flux linkage vectors onto the corresponding axes α, β, γ; ω_r – angular velocity of rotation of the rotor shaft.

Flux linkage in (2) [5]:

$$\begin{cases} \psi_{s\alpha} = L_{s\alpha}\cdot i_{s\alpha} + L\cdot\left(i_{r\alpha} - \dfrac{i_{r\beta}}{2} - \dfrac{i_{r\gamma}}{2}\right) - \dfrac{L\cdot i_{s\beta}}{2} - \dfrac{L\cdot i_{s\gamma}}{2}; \\ \psi_{s\beta} = L_{s\beta}\cdot i_{s\beta} + L\cdot\left(i_{r\beta} - \dfrac{i_{r\alpha}}{2} - \dfrac{i_{r\gamma}}{2}\right) - \dfrac{L\cdot i_{s\alpha}}{2} - \dfrac{L\cdot i_{s\gamma}}{2}; \\ \psi_{s\gamma} = L_{s\gamma}\cdot i_{s\gamma} + L\cdot\left(i_{r\gamma} + \dfrac{i_{r\alpha}}{2} + \dfrac{i_{r\beta}}{2}\right) - \dfrac{L\cdot i_{s\alpha}}{2} - \dfrac{L\cdot i_{s\beta}}{2}; \\ \psi_{r\alpha} = L_{r\alpha}\cdot i_{r\alpha} + L\cdot\left(i_{s\alpha} + \dfrac{i_{s\beta}}{2} + \dfrac{i_{s\gamma}}{2}\right) - \dfrac{L\cdot i_{r\beta}}{2} - \dfrac{L\cdot i_{r\gamma}}{2}; \\ \psi_{r\beta} = L_{r\beta}\cdot i_{r\beta} + L\cdot\left(i_{s\beta} + \dfrac{i_{s\alpha}}{2} + \dfrac{i_{s\gamma}}{2}\right) - \dfrac{L\cdot i_{r\gamma}}{2} - \dfrac{L\cdot i_{r\alpha}}{2}; \\ \psi_{r\gamma} = L_{r\gamma}\cdot i_{r\gamma} + L\cdot\left(i_{s\gamma} + \dfrac{i_{s\alpha}}{2} + \dfrac{i_{s\beta}}{2}\right) - \dfrac{L\cdot i_{r\alpha}}{2} - \dfrac{L\cdot i_{r\beta}}{2}, \end{cases} \quad (3)$$

where L is the mutual inductance.

Electromagnetic energy that is concentrated in the air gap of the machine [4]

$$W_5 = \frac{1}{2}\cdot\sum_{i=1}^{n}\psi_i\cdot i_i, \quad (4)$$

where $i = 1, 2, \ldots, n$ – number of windings in the machine.

Electromagnetic moment [5]

$$M = p\cdot\frac{\sqrt{3}}{2}\cdot L\cdot\left(\begin{matrix} i_{s\alpha}\cdot i_{r\gamma} + i_{s\beta}\cdot i_{r\alpha} + i_{s\gamma}\cdot i_{r\beta} - \\ -i_{s\alpha}\cdot i_{r\beta} - i_{s\beta}\cdot i_{r\gamma} - i_{s\gamma}\cdot i_{s\alpha} \end{matrix}\right), \quad (5)$$

where p is the number of pole pairs of the machine.

The set of equations (2) to (5) describes the processes of electromechanical energy conversion in a three-phase induction machine in the coordinate axes α, β, γ. The general system consists of fourteen equations, the dependent variables in it are six currents, six flux linkages, electromagnetic torque, and rotor rotation speed. The system is generally nonlinear since it contains equations in which the coefficients are functions of the dependent variables.

Expression (2) contains all possible pairs of current formation that determine the value of the electromagnetic torque. These pairs of currents generate vibrations in a real machine.

Assuming that the modulus of the flux linkage vector in the air gap of the machine ψ_δ depends only on the modulus of the resultant magnetodynamic force or on the magnetizing current i_μ proportional to it, the most complete consideration of saturation in dynamics was considered in works [4, 5]. The Filz method is based on the fact that when entering a nonlinear section of the magnetization curve of an induction machine, an increase in the magnetization current along one axis of the coordinate system causes a corresponding increase in the flux linkage ψ_δ along all axes of the specified system. Then it is possible to introduce the concepts of dynamic inductances along the axes and mutual inductances between the axes, which depend on the increase in the modules of the flux linkage vectors and the magnetization current and their spatial position.

In [4], the concept of the radial component of the dynamic inductance is introduced. It is the limiting value of the ratio of the increment of the flux linkage value to the increment of the magnetization current value when the magnetization current tends to zero

$$L_\rho^\partial = \frac{d\psi_\delta}{di_\mu}. \quad (6)$$

Similarly, in [5], the concept of the tangential component of dynamic inductance was introduced. It is the limiting value of the ratio of the increment of the working flux linkage to the increment of the magnetizing current if the magnetizing current tends to zero. In this case, the modulus of the magnetizing current vector remains constant

$$L_\tau^\partial = \frac{\psi_\delta}{i_\mu}. \quad (7)$$

Let us introduce the values inverse of the radial component of dynamic inductance

$$Y_\rho^\partial = \frac{1}{L_\rho^\partial} = \frac{di_\mu}{d\psi_\delta}, \quad (8)$$

and the tangential component of dynamic inductance

$$Y_\tau^\partial = \frac{1}{L_\tau^\partial} = \frac{i_\mu}{\psi_\delta}. \quad (9)$$

Their further use will simplify the mathematical form of recording the resulting ratios.

5. Results of investigating the mathematical model of a traction induction motor

5. 1. Accounting for the saturation of magnetic circuits in the mathematical description of an induction motor for a vessel's propulsion power plant

The systems of equations (2), (3), and (5) are supplemented with expressions that take into account the saturation of the machine's magnetic circuit.

After substituting expressions (3) into system (2), we obtain the voltage equation of the generalized machine in the braked three-phase coordinates.

For the α, β, γ coordinate system, the stator voltage equation taking into account losses in the steel will take the following form:

$$\begin{cases} u_{s\alpha} = i_{s\alpha} \cdot r_{s\alpha} + i_{\mu\alpha} \cdot r_{\mu} + \dfrac{d\psi_{s\alpha}}{dt}; \\ u_{s\beta} = i_{s\beta} \cdot r_{s\beta} + i_{\mu\beta} \cdot r_{\mu} + \dfrac{d\psi_{s\beta}}{dt}; \\ u_{s\gamma} = i_{s\gamma} \cdot r_{s\gamma} + i_{\mu\gamma} \cdot r_{\mu} + \dfrac{d\psi_{s\gamma}}{dt}, \end{cases} \quad (10)$$

where r_{μ} is the resistance equivalent to the losses in the steel; $i_{\mu\alpha}$, $i_{\mu\beta}$, $i_{\mu\gamma}$ are the projections of the magnetizing current vector.

Equation of the circuits of a squirrel-cage rotor:

$$\begin{cases} i_{r\alpha} \cdot r_{r\alpha} + \dfrac{d\psi_{r\alpha}}{dt} + \dfrac{\sqrt{3} \cdot \omega_r}{3} \cdot \left(\psi_{r\beta} - \psi_{r\gamma}\right) = 0; \\ i_{r\beta} \cdot r_{r\beta} + \dfrac{d\psi_{r\beta}}{dt} + \dfrac{\sqrt{3} \cdot \omega_r}{3} \cdot \left(\psi_{r\gamma} - \psi_{r\alpha}\right) = 0; \\ i_{r\gamma} \cdot r_{r\gamma} + \dfrac{d\psi_{r\gamma}}{dt} + \dfrac{\sqrt{3} \cdot \omega_r}{3} \cdot \left(\psi_{r\alpha} - \psi_{r\beta}\right) = 0. \end{cases} \quad (11)$$

According to the approach from [4], the flux linkage vector consists of the sum of the flux linkage vectors of the self-inductance and mutual inductance of the corresponding windings. Then the following expressions hold for the flux linkages:

$$\psi_{s\alpha} = \psi_{\sigma s\alpha} + \psi_{\delta\alpha}, \quad (12)$$

$$\psi_{s\beta} = \psi_{\sigma s\beta} + \psi_{\delta\beta}, \quad (13)$$

$$\psi_{s\gamma} = \psi_{\sigma s\gamma} + \psi_{\delta\gamma}, \quad (14)$$

$$\psi_{r\alpha} = \psi_{\sigma r\alpha} + \psi_{\delta\alpha}, \quad (15)$$

$$\psi_{r\beta} = \psi_{\sigma r\beta} + \psi_{\delta\beta}, \quad (16)$$

$$\psi_{r\gamma} = \psi_{\sigma r\gamma} + \psi_{\delta\gamma}, \quad (17)$$

where:

$$\psi_{\sigma s\alpha} = L_{\sigma s\alpha} \cdot i_{s\alpha}, \quad (18)$$

$$\psi_{\sigma s\beta} = L_{\sigma s\beta} \cdot i_{s\beta}, \quad (19)$$

$$\psi_{\sigma s\gamma} = L_{\sigma s\gamma} \cdot i_{s\gamma}, \quad (20)$$

$$\psi_{\sigma r\alpha} = L_{\sigma r\alpha} \cdot i_{r\alpha}, \quad (21)$$

$$\psi_{\sigma r\beta} = L_{\sigma r\beta} \cdot i_{r\beta}, \quad (22)$$

$$\psi_{\sigma r\gamma} = L_{\sigma r\gamma} \cdot i_{r\gamma}. \quad (23)$$

Projections of the magnetization current vector [5]:

$$i_{\mu\alpha} = i_{s\alpha} + i_{r\alpha}, \quad (24)$$

$$i_{\mu\beta} = i_{s\beta} + i_{r\beta}, \quad (25)$$

$$i_{\mu\gamma} = i_{s\gamma} + i_{r\gamma}. \quad (26)$$

Substitution of ratios (12) to (26) into system (10), after analytical transformations, allows us to obtain the following system of equations for stator windings:

$$\begin{cases} u_{s\alpha} = i_{s\alpha} \cdot r_{s\alpha} + i_{s\alpha} \cdot r_{\mu} + i_{r\alpha} \cdot r_{\mu} + L_{\sigma s\alpha} \cdot \dfrac{di_{s\alpha}}{dt} + \dfrac{d\psi_{\delta\alpha}}{dt}; \\ u_{s\beta} = i_{s\beta} \cdot r_{s\beta} + i_{s\beta} \cdot r_{\mu} + i_{r\beta} \cdot r_{\mu} + L_{\sigma s\beta} \cdot \dfrac{di_{s\beta}}{dt} + \dfrac{d\psi_{\delta\beta}}{dt}; \\ u_{s\gamma} = i_{s\gamma} \cdot r_{s\gamma} + i_{s\gamma} \cdot r_{\mu} + i_{r\gamma} \cdot r_{\mu} + L_{\sigma s\gamma} \cdot \dfrac{di_{s\gamma}}{dt} + \dfrac{d\psi_{\delta\gamma}}{dt}. \end{cases} \quad (27)$$

Similarly, substituting ratios (12) to (26) into system (11), after analytical transformations, allows us to obtain the following system of equations for the windings of a short-circuited rotor:

$$\begin{cases} i_{r\alpha} \cdot r_{r\alpha} + \dfrac{d\psi_{\delta\alpha}}{dt} + L_{\sigma r} \cdot \dfrac{di_{r\alpha}}{dt} + \dfrac{\sqrt{3} \cdot \omega_r}{3} \times \\ \times \left(L_{\sigma r} \cdot i_{r\beta} + \psi_{\delta\beta} - \left(L_{\sigma r} \cdot i_{r\gamma} + \psi_{\delta\gamma}\right)\right) = 0; \\ i_{r\beta} \cdot r_{r\beta} + \dfrac{d\psi_{\delta\beta}}{dt} + L_{\sigma r} \cdot \dfrac{di_{r\beta}}{dt} + \dfrac{\sqrt{3} \cdot \omega_r}{3} \times \\ \times \left(L_{\sigma r} \cdot i_{r\gamma} + \psi_{\delta\gamma} - \left(L_{\sigma r} \cdot i_{r\alpha} + \psi_{\delta\alpha}\right)\right) = 0; \\ i_{r\gamma} \cdot r_{r\gamma} + \dfrac{d\psi_{\delta\gamma}}{dt} + L_{\sigma r} \cdot \dfrac{di_{r\gamma}}{dt} + \dfrac{\sqrt{3} \cdot \omega_r}{3} \times \\ \times \left(L_{\sigma r} \cdot i_{r\alpha} + \psi_{\delta\alpha} - \left(L_{\sigma r} \cdot i_{r\beta} + \psi_{\delta\beta}\right)\right) = 0. \end{cases} \quad (28)$$

For the projections of vector i_{μ} based on relations (24) to (26) we can write the following:

$$\begin{cases} i_{\mu\alpha} = i_{s\alpha} + i_{r\alpha} = i_{\mu} \cdot \dfrac{\psi_{\delta\alpha}}{\psi_{\delta}}; \\ i_{\mu\beta} = i_{s\beta} + i_{r\beta} = i_{\mu} \cdot \dfrac{\psi_{\delta\beta}}{\psi_{\delta}}; \\ i_{\mu\gamma} = i_{s\gamma} + i_{r\gamma} = i_{\mu} \cdot \dfrac{\psi_{\delta\gamma}}{\psi_{\delta}}. \end{cases} \quad (29)$$

Or in differential form:

$$\begin{cases} \dfrac{d}{dt} i_{\mu\alpha} = \dfrac{di_{\mu}}{dt} \cdot \dfrac{\psi_{\delta\alpha}}{\psi_{\delta}} + i_{\mu} \cdot \dfrac{d}{dt}\left(\dfrac{\psi_{\delta\alpha}}{\psi_{\delta}}\right); \\ \dfrac{d}{dt} i_{\mu\beta} = \dfrac{di_{\mu}}{dt} \cdot \dfrac{\psi_{\delta\beta}}{\psi_{\delta}} + i_{\mu} \cdot \dfrac{d}{dt}\left(\dfrac{\psi_{\delta\beta}}{\psi_{\delta}}\right); \\ \dfrac{d}{dt} i_{\mu\gamma} = \dfrac{di_{\mu}}{dt} \cdot \dfrac{\psi_{\delta\gamma}}{\psi_{\delta}} + i_{\mu} \cdot \dfrac{d}{dt}\left(\dfrac{\psi_{\delta\gamma}}{\psi_{\delta}}\right). \end{cases} \quad (30)$$

Given that the values of derivatives of flux linkages are equal to:

$$\begin{cases} \dfrac{d}{dt}\left(\dfrac{\psi_{s\alpha}}{\psi_{\delta}}\right) = \dfrac{\psi_{\delta} \cdot \dfrac{d\psi_{s\alpha}}{dt} - \psi_{s\alpha} \cdot \dfrac{d\psi_{\delta}}{dt}}{\psi_{\delta}^2}; \\ \dfrac{d}{dt}\left(\dfrac{\psi_{s\beta}}{\psi_{s}}\right) = \dfrac{\psi_{\delta} \cdot \dfrac{d\psi_{s\beta}}{dt} - \psi_{s\beta} \cdot \dfrac{d\psi_{\delta}}{dt}}{\psi_{\delta}^2}; \\ \dfrac{d}{dt}\left(\dfrac{\psi_{s\gamma}}{\psi_{s}}\right) = \dfrac{\psi_{\delta} \cdot \dfrac{d\psi_{s\gamma}}{dt} - \psi_{s\gamma} \cdot \dfrac{d\psi_{\delta}}{dt}}{\psi_{\delta}^2}, \end{cases} \quad (31)$$

and given

$$\frac{di_{\mu}}{dt} = \frac{di_{\mu}}{d\psi_{\delta}} \cdot \frac{d\psi_{\delta}}{dt}, \quad (32)$$

the following system holds:

$$\begin{cases} \dfrac{d}{dt} i_{\mu\alpha} = \dfrac{\psi_{\delta\alpha}}{\psi_\delta} \cdot \dfrac{d\psi_\delta}{dt} \cdot \left(Y_\rho^\partial - Y_\tau^\partial \right) + Y_\tau^\partial \cdot \dfrac{d\psi_{\delta\alpha}}{dt}; \\ \dfrac{d}{dt} i_{\mu\beta} = \dfrac{\psi_{\delta\beta}}{\psi_\delta} \cdot \dfrac{d\psi_\delta}{dt} \cdot \left(Y_\rho^\partial - Y_\tau^\partial \right) + Y_\tau^\partial \cdot \dfrac{d\psi_{\delta\beta}}{dt}; \\ \dfrac{d}{dt} i_{\mu\gamma} = \dfrac{\psi_{\delta\gamma}}{\psi_\delta} \cdot \dfrac{d\psi_\delta}{dt} \cdot \left(Y_\rho^\partial - Y_\tau^\partial \right) + Y_\tau^\partial \cdot \dfrac{d\psi_{\delta\gamma}}{dt}. \end{cases} \quad (33)$$

The modulus of the flux linkage vector in an orthogonal coordinate system can be written as follows [4]:

$$\begin{cases} \psi_\delta = \sqrt{\psi_{\delta x}^2 + \psi_{\delta\gamma}^2}; \\ \psi_{\delta x} = \dfrac{2}{3} \cdot \psi_\alpha - \dfrac{1}{3} \cdot \psi_\beta - \dfrac{1}{3} \cdot \psi_\gamma; \\ \psi_{\delta\gamma} = \dfrac{\sqrt{3}}{3} \cdot \left(\psi_\beta - \psi_\gamma \right). \end{cases} \quad (34)$$

Then

$$\psi_\delta = \frac{2}{3} \cdot \sqrt{\left(\begin{matrix} \psi_{\delta\alpha} + \psi_{\delta\beta} + \\ + \psi_{\delta\gamma} \end{matrix} \right)^2 - 3 \cdot \left(\begin{matrix} \psi_{\delta\alpha} \cdot \psi_{\delta\beta} - \psi_{\delta\alpha} \cdot \psi_{\delta\gamma} - \\ - \psi_{\delta\beta} \cdot \psi_{\delta\gamma} \end{matrix} \right)}. \quad (35)$$

For projections of rotor currents, based on system (29), the following relations hold:

$$\begin{cases} i_{r\alpha} = Y_\tau^\partial \cdot \psi_{\delta\alpha} - i_{s\alpha}; \\ i_{r\beta} = Y_\tau^\partial \cdot \psi_{\delta\beta} - i_{s\beta}; \\ i_{r\gamma} = Y_\tau^\partial \cdot \psi_{\delta\gamma} - i_{s\gamma}. \end{cases} \quad (36)$$

In accordance with expressions (8), (9), (29) to (36), Fig. 2 shows a graphical interpretation of the physical content of radial dynamic inductance.

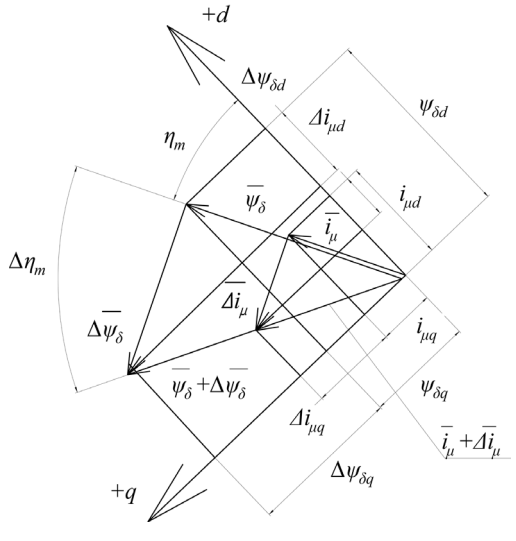

Fig. 2. Graphical interpretation of the physical meaning of radial dynamic inductance

In accordance with expressions (8), (9), (29) to (36), Fig. 3 shows a graphical interpretation of the physical meaning of tangential dynamic inductance.

The expression for electromagnetic moment takes the form

$$M = p \cdot \frac{\sqrt{3}}{2} \cdot \left(\begin{matrix} \psi_{\delta\alpha} \cdot \left(i_{s\beta} - i_{s\gamma} \right) + \\ + \psi_{\delta\beta} \cdot \left(i_{s\gamma} - i_{s\alpha} \right) + \psi_{\delta\gamma} \cdot \left(i_{s\alpha} - i_{s\beta} \right) \end{matrix} \right). \quad (37)$$

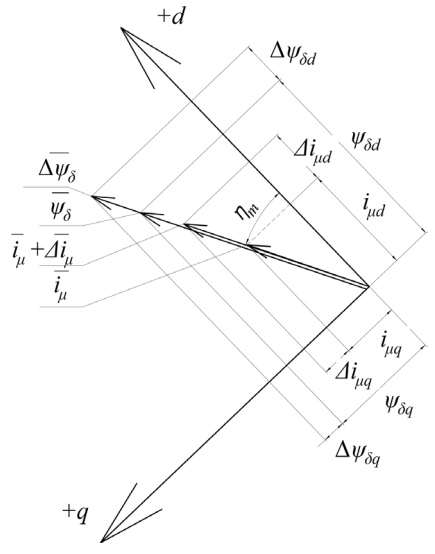

Fig. 3. Graphical interpretation of the physical meaning of tangential dynamic inductance

The equation of motion of the electromechanical part takes the following form [5]

$$\frac{d\omega_r}{dt} = p \cdot \frac{M + M_o}{J}, \quad (38)$$

where M_o is the reduced moment of resistance of the mechanism. Finally, the system of equations describing the processes of electromechanical energy conversion in a three-phase machine, in the coordinate axes α, β, γ taking into account saturation, is represented by the following system (39):

$$\begin{cases} u_{s\alpha} - i_{s\alpha} \cdot r_{s\alpha} - r_\mu \cdot \dfrac{i_\mu}{\psi_\delta} \cdot \psi_{\delta\alpha} - L_{\sigma s} \cdot \dfrac{di_{s\alpha}}{dt} = \\ = -r_{r\alpha} \cdot \left(i_{s\alpha} - \dfrac{i_\mu}{\psi_\delta} \cdot \psi_{\delta\alpha} \right) - L_{\sigma r} \cdot \dfrac{di_{r\alpha}}{dt} - \dfrac{\sqrt{3} \cdot \omega_r}{3} \times \\ \times \left(L_{\sigma r} \cdot \dfrac{di_\mu}{d\psi_\delta} \cdot \left(\psi_{\delta\beta} - \psi_{\delta\gamma} \right) + L_{\sigma r} \cdot \left(i_{s\gamma} - i_{s\beta} \right) + \psi_{\delta\beta} - \psi_{\delta\gamma} \right); \\ u_{s\beta} - i_{s\beta} \cdot r_{s\beta} - r_\mu \cdot \dfrac{i_\mu}{\psi_\delta} \cdot \psi_{\delta\beta} - \\ - L_{\sigma s} \cdot \dfrac{di_{s\beta}}{dt} - r_{r\beta} \cdot \left(i_{s\beta} - \dfrac{i_\mu}{\psi_\delta} \cdot \psi_{\delta\beta} \right) - \\ - L_{\sigma r} \cdot \dfrac{di_{r\beta}}{dt} - \dfrac{\sqrt{3} \cdot \omega_r}{3} \cdot \left(\begin{matrix} L_{\sigma r} \cdot \dfrac{di_\mu}{d\psi_\delta} \cdot \left(\psi_{\delta\gamma} - \psi_{\delta\beta} \right) + \\ + L_{\sigma r} \cdot \left(i_{s\alpha} - i_{s\gamma} \right) + \psi_{\delta\gamma} - \psi_{\delta\alpha} \end{matrix} \right); \\ u_{s\gamma} - i_{s\gamma} \cdot r_{s\gamma} - r_\mu \cdot \dfrac{i_\mu}{\psi_\delta} \cdot \psi_{\delta\gamma} - \\ - L_{\sigma s} \cdot \dfrac{di_{s\gamma}}{dt} - r_{r\gamma} \cdot \left(i_{s\gamma} - \dfrac{i_\mu}{\psi_\delta} \cdot \psi_{\delta\gamma} \right) - \\ - L_{\sigma r} \cdot \dfrac{di_{r\gamma}}{dt} - \dfrac{\sqrt{3} \cdot \omega_r}{3} \cdot \left(\begin{matrix} L_{\sigma r} \cdot \dfrac{di_\mu}{d\psi_\delta} \cdot \left(\psi_{\delta\alpha} - \psi_{\delta\beta} \right) + \\ + L_{\sigma r} \cdot \left(i_{s\beta} - i_{s\alpha} \right) + \psi_{\delta\alpha} - \psi_{\delta\beta} \end{matrix} \right); \\ \dfrac{d\omega_r}{dt} = p \cdot \dfrac{M + M_o}{J}; \\ \psi_\delta = \dfrac{2}{3} \cdot \sqrt{\left(\begin{matrix} \psi_{\delta\alpha} + \psi_{\delta\beta} + \\ + \psi_{\delta\gamma} \end{matrix} \right)^2 - 3 \cdot \left(\begin{matrix} \psi_{\delta\alpha} \cdot \psi_{\delta\beta} - \psi_{\delta\alpha} \cdot \psi_{\delta\gamma} - \\ - \psi_{\delta\beta} \cdot \psi_{\delta\gamma} \end{matrix} \right)}; \\ M = p \cdot \dfrac{\sqrt{3}}{2} \cdot \left(\begin{matrix} \psi_{\delta\alpha} \cdot \left(i_{s\beta} - i_{s\gamma} \right) + \psi_{\delta\beta} \cdot \left(i_{s\gamma} - i_{s\alpha} \right) + \\ + \psi_{\delta\gamma} \cdot \left(i_{s\alpha} - i_{s\beta} \right) \end{matrix} \right). \end{cases} \quad (39)$$

This system contains a set of differential and algebraic equations and unambiguously describes electromagnetic and electromechanical equations in a three-phase asynchronous machine, taking into account saturation.

5. 2. Verifying the model of an induction motor for a vessel's propulsion power plant taking into account the saturation of magnetic circuits

Taking as a basis the vessel's diesel-generator power plant Caterpillar 3516 (maximum power, 2500 kVA / 2000 kW; rated power, 2275 kVA / 1820 kW; generator type – Caterpillar 1844 with a rated frequency of 50 Hz.), a bench verification of the use of this mathematical model in the control system of a vessel's propulsion power plant was carried out (Fig. 4, 5).

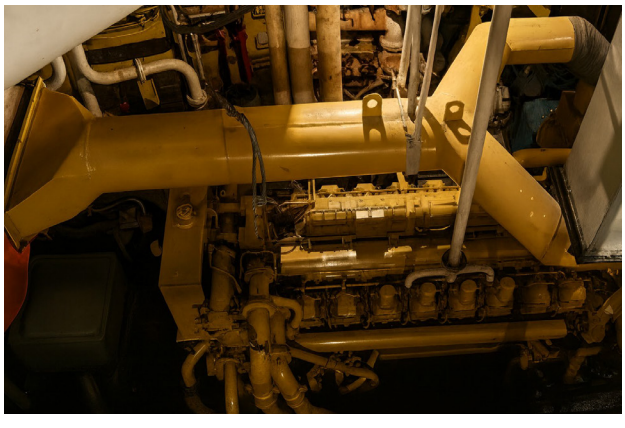

Fig. 4. Diesel generator of the vessel's propulsion power plant Caterpillar 3516

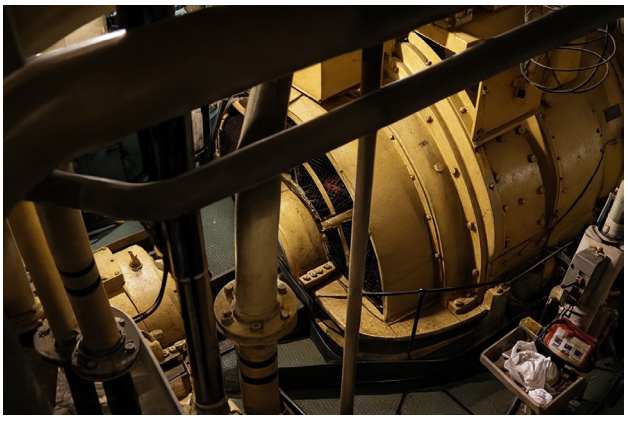

Fig. 5. Traction induction motor for the propeller drive of the vessel's propulsion power plant Caterpillar 3516

The verification was carried out on the basis of the power system, which is a combined power supply source for the ship's propulsion system and general transport electricity consumers (Fig. 6).

Our structural diagram describes one circuit in the power plant (diesel generator-rectifier-inverter-reducer-engine-motor), although it should be noted that the drive unit, as a rule, is multi-circuit. These circuits can function both independently and have a common bus of alternating or direct current. The power system provides power to consumers with three-phase current. The power sources are the main and backup diesel generators or an external voltage source, in particular an external transformer substation (for port operation). At the same time, it must have a power not less than the rated power of the single transport energy system, equipped with lightning protection and a dead-earthed neutral. This is typical for the docking mode or power supply from external vessels in the event of an accident. When powered from an external source, the voltage of the supply network through the protection circuit and filters is supplied to the rectifier. The rectifier performs the functions of voltage rectification, ripple smoothing, ensuring a smooth charging mode of the filter capacitors when the source is connected, as well as uninterrupted power supply to the load during short-term voltage drops in the network. In addition, the use of a filter reduces the level of interference. At the output of the network rectifier, a DC voltage is formed, which is within the rated values. Then, using a controlled inverter, this DC voltage is converted into AC.

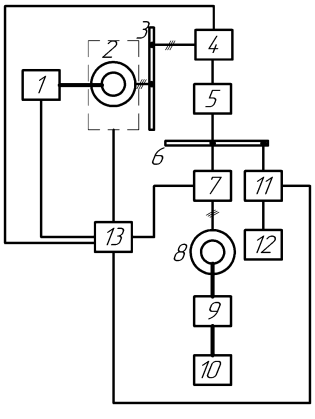

Fig. 6. Structural diagram of the power circuit in a vessel's power system: 1 – primary heat engine (mostly diesel); 2 – synchronous generator (the dotted line indicates the synchronous generator-exciter system); 3 – common AC bus; 4 – rectifier; 5 – DC filter unit; 6 – common DC bus; 7 – autonomous voltage inverter; 8 – induction machine; 9 – reducer; 10 – engine; 11 – converter for natural needs; 12 – consumers for natural needs; 13 – control system

To implement the frequency converter control system, we shall write its key switching function. The algorithm for implementing this function is as follows: the specified function will be equal to one if the corresponding power module of the frequency converter is open, and equal to zero if the corresponding power module of the frequency converter is open.

The design of the automatic voltage regulation circuit of the Caterpillar 3516 power plant is based on IGBT-type power modules. This is due to a number of advantages over other types of circuits for power systems:

– lower capacitance;
– simple control circuit;
– the ability to block control;
– higher operating frequency.

In this case, the autonomous voltage inverter is connected to a common DC bus, which is shunted by a capacitor filter designed to compensate for the reactive power of the load, and its use is a specific feature of this circuit.

The circuit of the autonomous voltage inverter contains six power modules, each of which is shunted by a corresponding diode. This configuration is necessary to ensure the conductivity of the current of the active-inductive load, which is a traction induction motor. The conversion of DC voltage into three-phase AC is carried out by sequentially switching the corresponding transistors. It is important that at any given

time in each of the inverter phases, three transistors must be simultaneously open, while the others remain closed.

The opening of the power switches occurs when a control pulse is received from the control system to the base (or gate) of the corresponding transistor. The quality and shape of the output AC voltage is determined by the specified parameters of the transistors. Under ideal conditions, it is possible to obtain a sinusoidal shape of the output AC voltage. Its frequency is regulated by increasing or decreasing the pulse frequency of the converter key. This ability to regulate the output voltage frequency is the key difference between a transistor voltage inverter and a thyristor inverter, which does not have such a function.

When using a power circuit with an isolated neutral of an autonomous voltage inverter, the algorithmic method of switching power keys can be described by the expressions given below.

For phase voltage AB:

$$U_{AB} = \begin{cases} \pm U_d \text{ if } S_1 \cdot S_4 \text{ or } S_2 \cdot S_3 = 1; \\ 0 \text{ if } S_1 \cdot S_3 = 1 \text{ or } S_2 \cdot S_4 = 1, \end{cases} \quad (40)$$

for phase voltage BC:

$$U_{BC} = \begin{cases} \pm U_d \text{ if } S_3 \cdot S_6 \text{ or } S_4 \cdot S_5 = 1; \\ 0 \text{ if } S_3 \cdot S_5 = 1 \text{ or } S_4 \cdot S_6 = 1, \end{cases} \quad (41)$$

for phase voltage CA:

$$U_{! A} = \begin{cases} \pm U_d \text{ if } S_5 \cdot S_2 \text{ or } S_6 \cdot S_1 = 1; \\ 0 \text{ if } S_1 \cdot S_5 = 1 \text{ or } S_2 \cdot S_6 = 1, \end{cases} \quad (42)$$

where U_{AB}, U_{BC}, U_{CA} are the corresponding phase voltages; S_1, S_2, S_3, S_4, S_5, S_6 are the control signals of the corresponding modules of the autonomous voltage inverter.

In this case, the state for which the system is executed is unacceptable:

$$\begin{cases} S_1 \cdot S_2 = 1; \\ S_3 \cdot S_4 = 1; \\ S_5 \cdot S_6 = 1. \end{cases} \quad (43)$$

An extended description of the control sequence of the frequency converter modules can provide for parallel connection of two phases of the traction induction motor in series with the third phase. The other phases change state only in relation to the common DC bus. Therefore, the relationships given below apply.

For phase voltage AB:

$$U_{AB} = \begin{cases} \pm U_d, \text{if } S_1 \cdot S_4 \cdot S_5 \text{ or } S_2 \cdot S_3 \cdot S_6 = 1; \\ 0, \text{if } S_1 \cdot S_5 = 1, S_4 = 0 \text{ or } S_1 \cdot S_5 = 0, S_4 = 1, \end{cases} \quad (44)$$

for phase voltage BC:

$$U_{BC} = \begin{cases} \pm U_d, \text{if } S_3 \cdot S_5 \cdot S_2 \text{ or } S_4 \cdot S_1 \cdot S_6 = 1; \\ 0, \text{if } S_3 \cdot S_5 = 1, S_2 = 0 \text{ or } S_3 \cdot S_5 = 0, S_2 = 1, \end{cases} \quad (45)$$

for phase voltage CA:

$$U_{CA} = \begin{cases} \pm U_d, \text{if } S_5 \cdot S_2 \cdot S_4 \text{ or } S_6 \cdot S_1 \cdot S_3 = 1; \\ 0, \text{if } S_4 \cdot S_2 = 1, S_5 = 0 \text{ or } S_2 \cdot S_4 = 0, S_5 = 1. \end{cases} \quad (46)$$

To ensure the software implementation of the switching function of the frequency converter, the following assumptions are adopted.

First, the power switches of the converter are considered ideal: their resistance in the open state is zero, the resistance in the closed state goes to infinity, and the switching time is instantaneous.

Second, when using pulse-width modulation, the switching time parameters (delays, rise time) are undesirably small compared to the actual duration of the conducting and non-conducting states of the corresponding switches.

Third, the values of the leakage currents through the closed switches are taken close to zero compared to the current in the open (working) position.

Fourth, during implementation, the ideality of the power source and switching elements is assumed, and the interval of the "dead" pause is also not taken into account.

While using the law of control over the keys of the power converter, it is necessary to determine the input and output parameters of the conversion of electrical energy, in particular, the quality of the output voltage. In this case, it should be taken into account that the sequence of behavior of the autonomous voltage inverter as a link in the closed automatic control system as a whole is of decisive importance. It is incorrect to take into account only the factors of the qualitative harmonic composition of the formed output voltage for powering the induction motor and ensuring a high efficiency.

The output parameters of the equivalent circuit of the motor are given in Table 1.

Table 1

Initial parameters of the equivalent motor circuit

Parameter	Parameter value
Rated power, W	240000
Rated phase stator voltage (rms), V	665
Rated phase stator current (rms), A	135
Rated rotor current (rms), A	128
Rated magnetizing current (rms), A	36
Rated phase starting current, A	300
Nominal current frequency, Hz	33.8
Maximum stator voltage frequency, Hz	95
Nominal rotor speed, rpm	10^3
Nominal absolute slip, s	0.02
Rotor moment of inertia, kg · m^2	21
Nominal torque, N · m	2366
Active stator resistance, Ohm	$83 \cdot 10^{-3}$
Active rotor resistance, Ohm	$68 \cdot 10^{-3}$
Rotor time constant (electromagnetic), s	1.294
Efficiency factor, s	0.937

As a result, the transient characteristics shown in Fig. 7 are obtained.

Based on the oscillograms shown in Fig. 7, a smooth increase in the rotor speed to 1000 rpm is observed during acceleration for approximately 0.2 s, which indicates high-quality dynamic controllability of the system. The stator current under a transient mode reaches a value of 300 A, while the current along the *y*-axis has an amplitude of about 280 A and repeats the shape of the main current, which indicates the dominance of the reactive component in the magnetization process. The rotor magnetic flux increases to 9 Vb with noticeable oscillations at the beginning of the start-up, which

quickly fade away, and then settles at the level of 6–7 Vb. During braking, a mirror-shaped process occurs, characterized by the symmetry of the electromechanical characteristics of the motor.

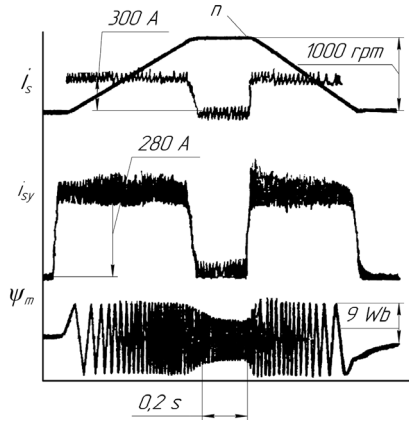

Fig. 7. Oscillograms of a full-scale experiment

Our results indicate a stable aperiodic nature of transient processes, the absence of supersaturation of the magnetic circuit, and effective damping of oscillations. This confirms the high-quality dynamics of the induction motor and the suitability of the control system for fast reversing modes taking into account magnetic processes.

6. Results of investigating the saturation processes in an induction machine: discussion and summary

Our results, represented in the form of a system of equations (39), including four differential and two algebraic equations, are a direct consequence of the application of the method of dynamic inductances based on a generalized spatial model (Fig. 1). Such a compact structure of the system is explained by the effectiveness of the introduction of radial and tangential dynamic inductances (6), (7), which make it possible to integrate nonlinear dependences of the magnetic circuit. This provided the possibility for correctly reflecting the variability of the magnetic state of the engine in a wide range of loads, since dynamic inductances quantitatively reflect nonlinear changes in parameters due to saturation (Fig. 2, 3).

The verification results obtained on the basis of the Caterpillar 3516 vessel power plant (Fig. 4, 5), which are displayed on the oscillograms (Fig. 7), confirm the adequacy and completeness of the built model. The observed stable aperiodic nature of transient processes and the smooth increase in speed indicate that the model accurately reflects the dynamics of a powerful machine, ensuring full control over processes in linear and nonlinear sections of the magnetization characteristic.

The advantages of this study are attributed to the comprehensive consideration of saturation and cross-saturation while maintaining the numerical efficiency of the model. Unlike approaches based on field magnetic models, which are computationally complex and require detailed geometric data, our compact system (39) allows for an adequate description of the dynamics while minimizing computational resources. This becomes possible due to the use of the dynamic inductance method, which effectively integrates nonlinear parameters into the spatial model. In addition, unlike a significant part of known solutions that do not take cross-saturation into account or are tested on low-power machines, the model built takes into account the relationship of flows and currents in different coordinate axes. The model has been verified on a high-power traction machine, which confirms its feasibility for the class of propeller traction engines.

The scientific and applied task of taking into account the saturation processes has been solved by integrating dynamic inductances, which allowed us to take into account the saturation of the main magnetic circuit and cross-saturation. Relations (27) and (28) for the stator and rotor windings confirm the possibility of taking into account nonlinearities within a compact system of equations.

Successful verification on a real installation (Fig. 7) shows that the model provides accurate reproduction of actual physical processes and effective control over transient processes.

A special feature of the proposed mathematical model of a traction induction motor is the comprehensive consideration of the processes of magnetic saturation, cross-saturation, and losses in steel. At the same time, the numerical efficiency and compactness of the system of equations are preserved. Unlike detailed field magnetic models (FEA) [1–5], the proposed approach does not require detailed geometric data of the machine and complex calculations. The resulting compact system of equations contains four differential and two algebraic equations and provides an adequate description of the dynamics at minimal computational costs. This was made possible by the method of dynamic inductances, which integrates nonlinear parameters into the spatial model.

Unlike known solutions [6, 8, 12] that ignore cross-saturation or describe it in a simplified manner, our model takes into account the relationship of fluxes and currents in different coordinate axes. This allows for a more accurate reproduction of magnetic phenomena in powerful traction machines with large currents. This result was possible thanks to the application of the method of dynamic inductances (Filtz method). This method makes it possible to accurately determine the change in inductances during the saturation process.

An important feature of the model is its experimental verification. Unlike works [24, 27, 31], which verify the models on laboratory or medium-sized machines, our verification was performed on a shipboard installation Caterpillar 3516. This confirms the transferability of the model to high-power propeller traction engines. Our results demonstrate the ability of the model to accurately reproduce real processes under operating conditions of vessel systems.

Thus, unlike conventional mathematical models that do not fully reflect the effects of saturation, the proposed system of equations with dynamic inductances provides an adequate description of transient regimes. It is suitable for studying and controlling high-power marine power plants.

When attempting to apply it in practice and in further theoretical studies, it is necessary to take into account the following limitations of this study. The proposed solutions are adequate within the framework of a stable thermal regime of the engine. A change in the thermal state of the machine leads to a change in the indicators of the equivalent circuit, which can reduce the accuracy of using the model, so this must be taken into account in its practical operation. In addition, the accuracy of predicting dynamics depends on the availability of reliable experimental data for identifying saturation parameters. This imposes restrictions on the need to re-identify parameters when changing the magnetic properties of steels, which can occur due to aging of materials.

Despite the above limitations, there are also shortcomings of the study that may make it impossible to provide practical or theoretical expectations from using the results, even under the specified conditions. A potential drawback is that the design does not cover other nonlinear processes, such as hysteresis and frequency-dependent losses (steel losses). Ignoring these effects may lead to the impossibility of ensuring the accuracy of energy loss estimation and the adequacy of dynamics modeling during ultrafast transients. This is because these unaccounted processes significantly affect the overall magnetic state and machine parameters at high flux change frequencies, which is uncharacteristic for transport power plants.

Further studies in this area should tackle two key directions. The first is the integration of the thermal module into the constructed system of equations. This is necessary because such an extension will make it possible to increase the accuracy of the model and its adequacy under conditions of long-term and sharply changing loads of marine transport, ensuring dynamic correction of the parameters of the equivalent circuit depending on the temperature. The second promising direction is the combination of saturation with hysteresis and frequency-dependent losses within the same model. This will make it possible to devise a systematic and complete approach for simultaneously taking into account all the main nonlinearities in models suitable for real-time control systems with high-power engines.

7. Conclusions

1. We have built a system of mathematical equations that describes electromechanical and electromagnetic processes in the circuits of an induction motor of a vessel's propulsion power plant, taking into account the saturation of magnetic circuits. The indicated relations contain four differential and two algebraic equations, which is sufficient to determine the full controllability of dynamics in linear and nonlinear sections of the magnetization characteristic. This became possible due to the use of the method of dynamic inductances as the main tool in building a mathematical model.

2. The verification of the model of an induction motor of a vessel's propulsion power plant, taking into account the saturation of magnetic circuits, showed that our results are acceptable in the development and construction of drive control systems and auto guidance systems. This became possible due to the consideration of the change in the magnetic state of the traction induction machine, which allowed us to describe, adequately to real electromagnetic and electromechanical processes, the induction machine, as well as simulate the specified processes. The mathematical model built shows positive prospects for further research in this area to derive more accurate relations describing the circuits of a traction induction motor based on the obtained equations.

Conflicts of interest

The authors declare that they have no conflicts of interest in relation to the current study, including financial, personal, authorship, or any other, that could affect the study, as well as the results reported in this paper.

Funding

The study was conducted without financial support.

Data availability

All data are available, either in numerical or graphical form, in the main text of the manuscript.

Use of artificial intelligence

The authors declare the use of generative AI in the research and manuscript preparation process. According to the GAIDeT taxonomy (2025), the following tasks were delegated to generative AI tools under full human supervision:

– Literature search and systematization.

– Assessment of research novelty and identification of gaps.

Generative AI tool used: Gemini 2.5.

The authors bear full responsibility for the final manuscript.

Generative AI tools are not credited as authors and are not responsible for the final results.

Declaration submitted by: Collective responsibility.

Acknowledgments

The authors express their gratitude to the Armed Forces of Ukraine for protection, the opportunity to work, and be free.

Authors' contributions

Dmytro Kulagin: Conceptualization, Funding acquisition, Investigation, Methodology, Project administration, Writing – review & editing; **Igor Maslov**: Data curation, Formal analysis, Resources, Software, Supervision, Validation, Visualization, Writing – original draft.

References

1. Maslov, I., Tymoshchuk, O., Kulagin, D. (2025). Determining the causes of major energy losses in a ship's unified AC power system. Modern Automotive Industry, Transport And Road Infrastructure '2024 (MAITRI2024), 3428, 020021. https://doi.org/10.1063/12.0038611
2. Kulagin, D., Maslov, I. (2024). Mathematical Model of Electromagnetic Transients of a Frequency-Controlled Propeller's Induction Motor. 2024 IEEE 5th KhPI Week on Advanced Technology (KhPIWeek), 1–5. https://doi.org/10.1109/khpiweek61434.2024.10877991
3. Kulahin, D. O. (2016). Rolling electrical complex on the basis of the criterion of minimizing the area under the curve of motion. Naukovyi Visnyk Natsionalnoho Hirnychoho Universytetu, 2, 60–67. Available at: https://nvngu.in.ua/index.php/en/archive/on-the-issues/1214-2016/contents-no-2-2016/electrical-complexes-and-systems/3396-rolling-electrical-complex-on-the-basis-of-the-criterion-of-minimizing-the-area-under-the-curve-of-motion

4. Kulagin, D. O. (2014). The mathematical model of asynchronous traction motor taking into account the saturation of magnetic circuits. Naukovyi Visnyk Natsionalnoho Hirnychoho Universytetu, 6, 103–110. Available at: https://nvngu.in.ua/index.php/en/archive/on-the-issues/1012-2014/contents-no-6-2014/electrical-complexes-and-systems/2867-the-mathematical-model-of-asynchronous-traction-motor-taking-into-account-the-saturation-of-magnetic-circuits
5. Kulagin, D. O. (2014). Mathematical model of asynchronous traction motor taking into account the saturation. Technical Electrodynamics, 6, 49–55. Available at: https://techned.org.ua/index.php/techned/article/view/1126/1001
6. Konuhova, M. (2024). Modeling of Induction Motor Direct Starting with and without Considering Current Displacement in Slot. Applied Sciences, 14 (20), 9230. https://doi.org/10.3390/app14209230
7. Gupta, V. K., Samanta, P., Sahay, P. K., Srinivas, V. L. (2025). From Conveyor Belts to Crushers: A Review on Radial and Axial Flux Induction Motor Advances and Applications in Industrial Mining Operations. 2025 IEEE 1st International Conference on Smart and Sustainable Developments in Electrical Engineering (SSDEE), 01–06. https://doi.org/10.1109/ssdee64538.2025.10968154
8. Chen, H., Bi, C., Li, S., Peng, Z., Chen, Z. (2024). New Approach to Improve Starting Performance of Induction Motor Based on Optimal Starting Frequency. IEEE Access, 12, 136515–136523. https://doi.org/10.1109/access.2024.3463424
9. Larabee, J., Pellegrino, B., Flick, B. (2005). Induction Motor Starting Methods and Issues. Record of Conference Papers Industry Applications Society 52nd Annual Petroleum and Chemical Industry Conference, 217–222. https://doi.org/10.1109/pcicon.2005.1524557
10. Park, D.-H., Song, C.-H., Won, Y.-J., Park, J.-C., Kim, H.-S., Park, H.-R. et al. (2024). Magnetizing Inductance Estimation Method of Induction Motor for EV Traction Considering Magnetic Saturation Changes According to Current and Slip Frequency. IEEE Transactions on Magnetics, 60 (9), 1–5. https://doi.org/10.1109/tmag.2024.3426663
11. Masadeh, M. A., Amitkumar, K. S., Pillay, P. (2018). Power Electronic Converter-Based Induction Motor Emulator Including Main and Leakage Flux Saturation. IEEE Transactions on Transportation Electrification, 4 (2), 483–493. https://doi.org/10.1109/tte.2018.2824619
12. Accetta, A., Alonge, F., Cirrincione, M., D'Ippolito, F., Pucci, M., Sferlazza, A. (2017). GA-based off-line parameter estimation of the induction motor model including magnetic saturation and iron losses. 2017 IEEE Energy Conversion Congress and Exposition (ECCE), 2420–2426. https://doi.org/10.1109/ecce.2017.8096466
13. Zhang, Y., Baig, S., Vahabzadeh, T., Jatskevich, J. (2022). Maximum Efficiency Volts-per-Hertz Control of Induction Motor Drives Considering Core Losses, Saturation, and Inverter Losses. 2022 International Conference on Electrical, Computer and Energy Technologies (ICECET), 1–7. https://doi.org/10.1109/icecet55527.2022.9872679
14. Iegorov, O., Iegorova, O., Potryvaieva, N., Zaluzhna, H. (2021). The Traction Induction Motor Magnetic Circuit Saturation Influence on the Variable Electric Drive Energy Efficiency. 2021 IEEE International Conference on Modern Electrical and Energy Systems (MEES), 1–5. https://doi.org/10.1109/mees52427.2021.9598686
15. Siddique, A., Yadava, G. S., Singh, B. (2005). A Review of Stator Fault Monitoring Techniques of Induction Motors. IEEE Transactions on Energy Conversion, 20 (1), 106–114. https://doi.org/10.1109/tec.2004.837304
16. Jang, J.-H., Sul, S.-K., Jung-Ik Ha, Ide, K., Sawamura, M. (2003). Sensorless drive of surface-mounted permanent-magnet motor by high-frequency signal injection based on magnetic saliency. IEEE Transactions on Industry Applications, 39 (4), 1031–1039. https://doi.org/10.1109/tia.2003.813734
17. Palma Garcia, M. T., Caceres Cardenas, F. V., Kuong, J. L., Quispe, E. C. (2018). Transient Analysis of Induction Motors Considering the Saturation Effect Applying the Finite Element Method. 2018 IEEE ANDESCON, 1–6. https://doi.org/10.1109/andescon.2018.8564699
18. Kulagin, D. O., Fedosha, D. V., Nitsenko, V. V., Shevchenko, S. Yu., Danylchenko, D. O. (2019). Using a phase-differential busbar protection for switchgears of power system facilities. Naukovyi Visnyk Natsionalnoho Hirnychoho Universytetu, 4. https://doi.org/10.29202/nvngu/2019-4/10
19. Nitsenko, V., Kulagin, D. (2017). Improvement implementation methods of relay busbars protection of switchgears. Tekhnichna Elektrodynamika, 6, 61–71. https://doi.org/10.15407/techned2017.06.061
20. Nitsenko, V. V., Kulahin, D. O. (2017). Research on effect of differential-phase protection of busbars system with voltage of 110–750 kv. Naukovyi Visnyk Natsionalnoho Hirnychoho Universytetu, 4, 72–79. Available at: https://www.researchgate.net/publication/321157798_Research_on_effect_of_differential-phase_protection_of_busbars_system_with_voltage_of_110-750_kv
21. Korobko, B., Kivshyk, A., Kulagin, D. (2021). Experimental Study of the Efficiency of the Differential Pump of Electromagnetic Action on the Basis of Mathematical Modeling of the Parameters of Its Operation. Proceedings of the 3rd International Conference on Building Innovations, 203–213. https://doi.org/10.1007/978-3-030-85043-2_20
22. Bratkovska, K., Makhlin, P., Shram, A., Kulagin, D., Fedosha, D. (2022). Estimation of Optimization Approaches of the Energy Intensive Equipment's Power-Time Diagrams of Industrial Enterprises. 2022 IEEE 8th International Conference on Energy Smart Systems (ESS), 277–281. https://doi.org/10.1109/ess57819.2022.9969248
23. Yekimov, S., Nianko, V., Kulagin, D., Lunkina, T., Haponenko, S. (2021). The importance of environmental education for effective environmental management. E3S Web of Conferences, 296, 08002. https://doi.org/10.1051/e3sconf/202129608002
24. Masadeh, M. A., Pillay, P. (2017). Induction motor emulation including main and leakage flux saturation effects. 2017 IEEE International Electric Machines and Drives Conference (IEMDC), 1–7. https://doi.org/10.1109/iemdc.2017.8002207

25. Kulagin, D., Maslov, I., Lysechko, V., Prokopenko, V., Shram, A., Pastushenko, V. (2023). Analysis Of Current Approaches to Modernizing the Electric Power Scheme of Diesel Generator Transport. 2023 IEEE 4th KhPI Week on Advanced Technology (KhPIWeek), 1–6. https://doi.org/10.1109/khpiweek61412.2023.10312881
26. Molsa, E., Saarakkala, S. E., Hinkkanen, M. (2018). Influence of Magnetic Saturation on Modeling of an Induction Motor. 2018 XIII International Conference on Electrical Machines (ICEM), 1572–1578. https://doi.org/10.1109/icelmach.2018.8506746
27. Dalal, A., Singh, A. K., Kumar, P. (2013). Effect of saturation on equivalent circuit analysis of induction motor in practical scenario. 2013 Annual IEEE India Conference (INDICON), 1–5. https://doi.org/10.1109/indcon.2013.6726122
28. Nishihama, K., Ide, K., Mikami, H., Fujigaki, T., Mizutani, S. (2009). Starting torque analysis of cage induction motor using permeance model considering magnetic saturation by leakage flux. 2009 International Conference on Electrical Machines and Systems, 1–6. https://doi.org/10.1109/icems.2009.5382970
29. Novotnak, R. T., Chiasson, J., Bodson, M. (1999). High-performance motion control of an induction motor with magnetic saturation. IEEE Transactions on Control Systems Technology, 7 (3), 315–327. https://doi.org/10.1109/87.761052
30. Faiz, J., Ebrahimi, B. M., Toliyat, H. A. (2009). Effect of Magnetic Saturation on Static and Mixed Eccentricity Fault Diagnosis in Induction Motor. IEEE Transactions on Magnetics, 45 (8), 3137–3144. https://doi.org/10.1109/tmag.2009.2016416
31. Sprooten, J., Maun, J.-C. (2009). Influence of Saturation Level on the Effect of Broken Bars in Induction Motors Using Fundamental Electromagnetic Laws and Finite Element Simulations. IEEE Transactions on Energy Conversion, 24 (3), 557–564. https://doi.org/10.1109/tec.2009.2016126
32. Faiz, J., Ojaghi, M. (2011). Stator Inductance Fluctuation of Induction Motor as an Eccentricity Fault Index. IEEE Transactions on Magnetics, 47 (6), 1775–1785. https://doi.org/10.1109/tmag.2011.2107562
33. Kwon, S. O., Lee, J. J., Lee, B. H., Kim, J. H., Ha, K. H., Hong, J. P. (2009). Loss Distribution of Three-Phase Induction Motor and BLDC Motor According to Core Materials and Operating. IEEE Transactions on Magnetics, 45 (10), 4740–4743. https://doi.org/10.1109/tmag.2009.2022749
34. Fernandez-Bernal, F., Garcia-Cerrada, A., Faure, R. (2000). Model-based loss minimization for DC and AC vector-controlled motors including core saturation. IEEE Transactions on Industry Applications, 36 (3), 755–763. https://doi.org/10.1109/28.845050